Journal of Advances in Modeling Earth Systems

Supporting Information for

Towards Robust Parameterizations in Ecosystem-level Photosynthesis Models

Shanning Bao[1,2*], Lazaro Alonso[1], Siyuan Wang[1], Johannes Gensheimer[1], Ranit De[1], Nuno Carvalhais[1,3,4*]

[1]Department for Biogeochemical Integration, Max-Planck-Institute for Biogeochemistry, 07745, Jena, Germany.

[2]National Space Science Center, Chinese Academy of Sciences, 100190, Beijing, China.

[3]Departamento de Ciências e Engenharia do Ambiente, DCEA, Faculdade de Ciências e Tecnologia, FCT, Universidade Nova de Lisboa, 2829-516 Caparica, Portugal.

[4]ELLIS Unit Jena, 07745, Jena, Germany.

Contents of this file

Introduction

The supporting information includes the descriptions of model parameters calibration (text S1), cost functions used in SPIE (text S2), and figures and tables to supplement the information about the data and results appeared in the main text.

Text S1. Model parameters calibration

To get the highest model performance, we here calibrated the LUE model at each site using the full time series of GPP_{obs}. The purpose of model calibration is to find the parameter vector that can minimize the cost function, a metric to measure the model error, and to reduce

the model uncertainties associated with model parameters. In the calibration process, the parameters were optimized in their physical ranges (Table 1) using a stochastic and derivative-free evolutionary algorithm, CMAES(Hansen & Kern, 2004). CMAES, which is a reliable tool for global optimization (Trautmann et al., 2018).

We define the cost function (*cf*) as the sum of the GPP errors (cf_1, equation S- 2), the ET errors (cf_2, equation S- 3), and the environmental sensitivity functions (*f*X) constraints (cf_3 and cf_4).

$$cf = cf_1 + cf_2 + (cf_3 + cf_4) \quad S\text{-}1$$

$$cf_1 = \sum_{t=1}^{N_t} \sqrt{\left(GPP_t - \widehat{GPP}_t\right)^2 \cdot \sigma_{NEE_t}^{-2}} \quad S\text{-}2$$

$$cf_2 = \sum_{t=1}^{N_t} \sqrt{\left(ET_t - \widehat{ET}_t\right)^2 \cdot \sigma_{LE_t}^{-2}} \quad S\text{-}3$$

The cf_1 and cf_2 are to measure the sum of squares for errors of simulated GPP and ET, which is used to optimize the parameters of water availability index (WAI, see Table S2), at each time step *t*. The simulated GPP using the calibrated LUE parameters ($\widehat{GPP}$) and simulated ET using the calibrated WAI parameters ($\widehat{ET}$) were compared to GPP_{obs} (*GPP*) and ET_{obs} (*ET*), respectively. N_t denotes the total number of time steps. Due to the uncertainties in observation and the different units of GPP and ET, we weighted the model errors using the estimated uncertainty of *GPP* (σ_{NEE}) and *ET* (σ_{LE}), respectively. We assume that the parameter vector that minimizes the sum of cf_1 and cf_2 is the best for the LUE model and WAI, respectively.

We follow the concept of ecological and dynamic constraints (EDC, by (Bloom & Williams, 2015)) to regularize the inversion approach via two additional constraints: cf_3 (equation S- 4) and cf_4 (equation S- 5).

$$cf_3 = \left(\left(1\text{-}\max(f\mathrm{T}_r)\right) + \left(1\text{-}\max(f\mathrm{VPD}_r)\right) + \left(1\text{-}\max(f\mathrm{W}_r)\right) + \left(1\text{-}\max(f\mathrm{L}_r)\right)\right) \cdot c \quad S\text{-}4$$

$$cf_4 = \left(\sum_r \left(fT_r(T<0\,°C) > \theta_{fT}\right) + \sum_r \left(fVPD_r(VPD>2kPa) > \theta_{fVPD}\right) + \sum_r \left(fW_r(W<0.01) > \theta_{fW}\right)\right) \cdot c \quad S\text{-}5$$

These impose constraints on the simulated *f*X (i.e., *f*T, *f*VPD, *f*W, *f*L and *f*CI) based on two assumptions: the instantaneous ε ($=\varepsilon_{max} \cdot f\mathrm{T} \cdot f\mathrm{VPD} \cdot f\mathrm{W} \cdot f\mathrm{L} \cdot f\mathrm{CI}$) of vegetation can reach its potential, ε_{max}, under some specific environmental condition (cf_3) and is inhibited under a non-ideal growing condition (cf_4). Here cf_3 and cf_4 were calculated independently from cf_1 and cf_2, using analog inputs (PAR=0-20 $MJ \cdot m^{-2} \cdot day^{-1}$, FAPAR=0-1, T=-10-40 °C, VPD=0-2 kPa, W=0-1 and CI=0-1). *cf*3 is to set the maximum of *f*T, *f*VPD, excluding the CO_2 fertilization effect (the right part of equation 3), *f*W, and *f*L to one, which implies that the corresponding environmental factor does not limit ε at a certain point within the given ranges of PAR$\in$ [0,20] (in $MJ \cdot m^{-2} \cdot day^{-1}$), FAPAR$\in$[0,1], T$\in$[-10,40] (in °C), VPD$\in$[0,2] (in kPa), W$\in$[0,1] and CI$\in$[0,1], represented by the subscript, *r*, in equations S- 4-S- 5 (e.g., $\max(f\mathrm{T}_r)$ represents the maximum *f*T when the temperature is ranging between -10 and 40 °C).

Another constraint, cf_4, is to guarantee the *f*T, *f*VPD, excluding the CO_2 fertilization part, and *f*W lower than the threshold (θ_{fT}, θ_{fVPD}, and θ_{fW}) under the non-ideal conditions (T<0 °C, VPD>2 kPa, or W<0.01). Here the thresholds (θ_{fT}=0.2, θ_{fVPD}=0.9, and θ_{fW}=0.2) were estimated according to the normalized ratio of GPP to APAR at all sites. The other non-ideal conditions were not included since they vary across sites. The *c* in equations S- 4-S- 5 denotes a penalty term ($=10^4$, an empirical value) to coordinate the scales of cf_1, cf_2, cf_3, and cf_4.

Since the WAI parameters were not predicted in this study, the calibrated WAI parameters were used in the parameterization experiments and the cf_2 was not considered in the optimization-based parameterization methods, i.e., 'OPT-All' and 'OPT-PFT'.

Text S2. Cost functions used in SPIE

The cost function (cf_{NN}, equation S- 6) for SPIE was similar to the sum of cf_1, cf_3, and cf_4. Since normalizing the cost function can significantly improve the training efficiency of neural network, we used normalized NSE (Nossent & Bauwens, 2012), ranging from 0-1, rather than the sum of squares (S- 7).

$$cf_{NN}=cf_{NN1}+cf_3+cf_4 \qquad S\text{- }6$$

$$cf_{NN1}=\frac{\sum_{t=1}^{N_t}\left(GPP_t-\widehat{GPP}_t\right)^2\cdot\sigma_{NEE_t}{}^{-2}}{\sum_{t=1}^{N_t}\left(GPP_t-\widehat{GPP}_t\right)^2\cdot\sigma_{NEE_t}{}^{-2}+\sum_{t=1}^{N_t}\left(GPP_t-\overline{GPP}\right)^2\cdot\sigma_{NEE_t}{}^{-2}} \qquad S\text{- }7$$

GPP_t and $\widehat{GPP}_t$ are the observed and simulated GPP at time step, t. The normalized NSE is the ratio between the sum of the GPP errors across all time steps (N_t) to the sum of GPP errors and the sum of GPP changes to the average GPP ($\overline{GPP}$). To consider the EDC, we added cf_{NN1} to cf_3 and cf_4 as defined in section S1. The only difference was that the empirical coefficient, c, was changed to 0.2 here due to the small range of cf_{NN1}.

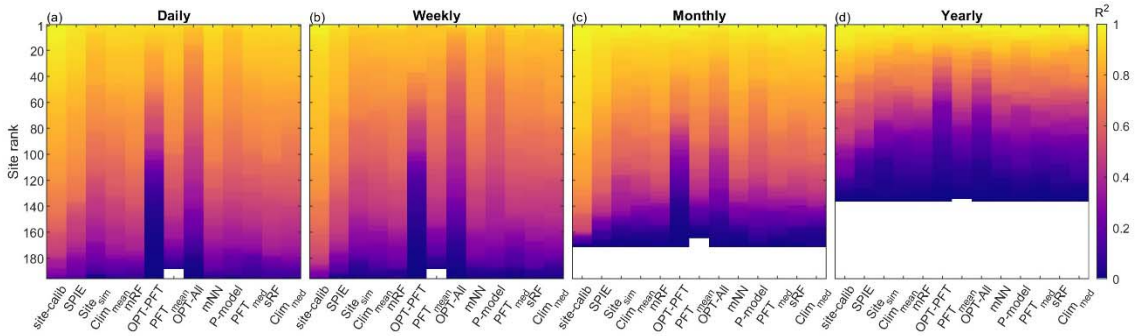

Figure S1. Comparison of R^2 between GPP_{obs} and GPP_{sim} based on twelve different parameterization methods, and between GPP_{obs} and GPP_{calib} (site-calib) at daily (a), weekly (b), monthly (c) and yearly (d) scales. The sites with less than four good-quality months or years are removed from panel c and d, respectively. The sites with p-value larger than 0.05 are shown in white.

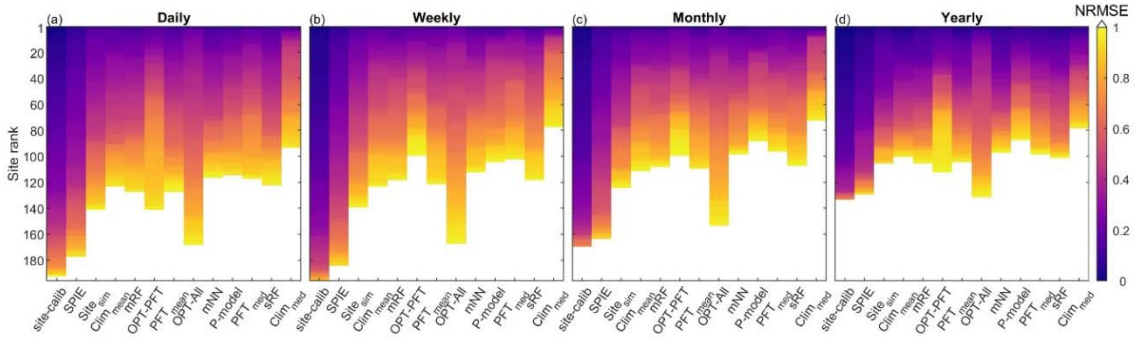

Figure S2. Comparison of NRMSE between GPP_{obs} and GPP_{sim} based on twelve different parameterization methods, and between GPP_{obs} and GPP_{calib} (site-calib) at daily (a), weekly (b), monthly (c) and yearly (d) scales.

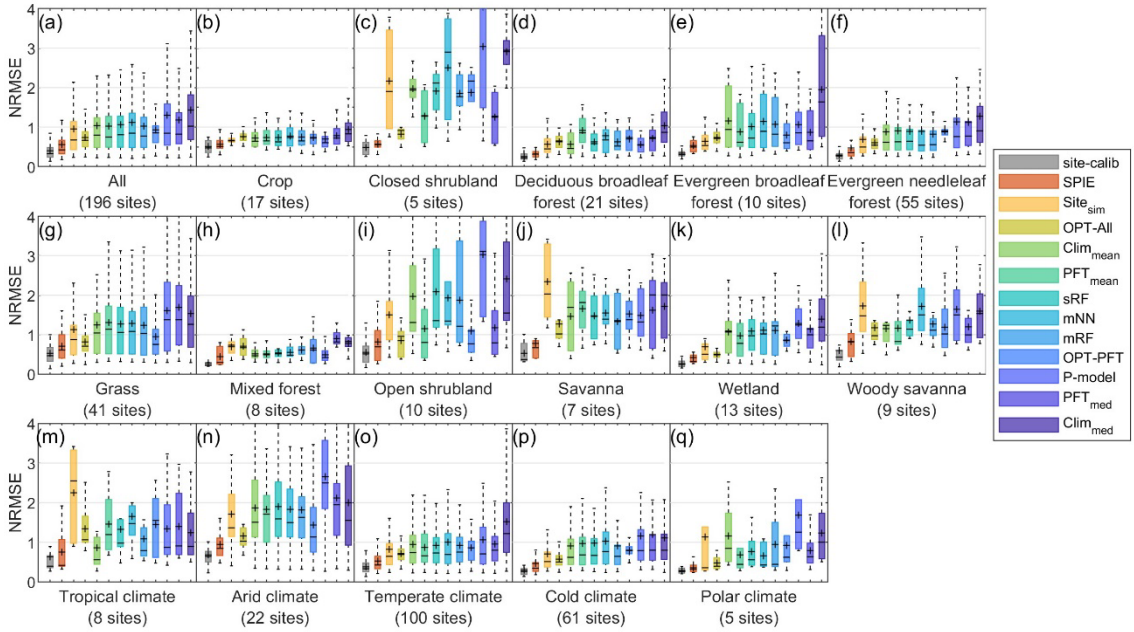

Figure S3. Site-level daily NRMSE comparison across all sites (a), per PFT (b-l) and per Clim (m-q). The mean and median per type are represented by the black cross and line, respectively

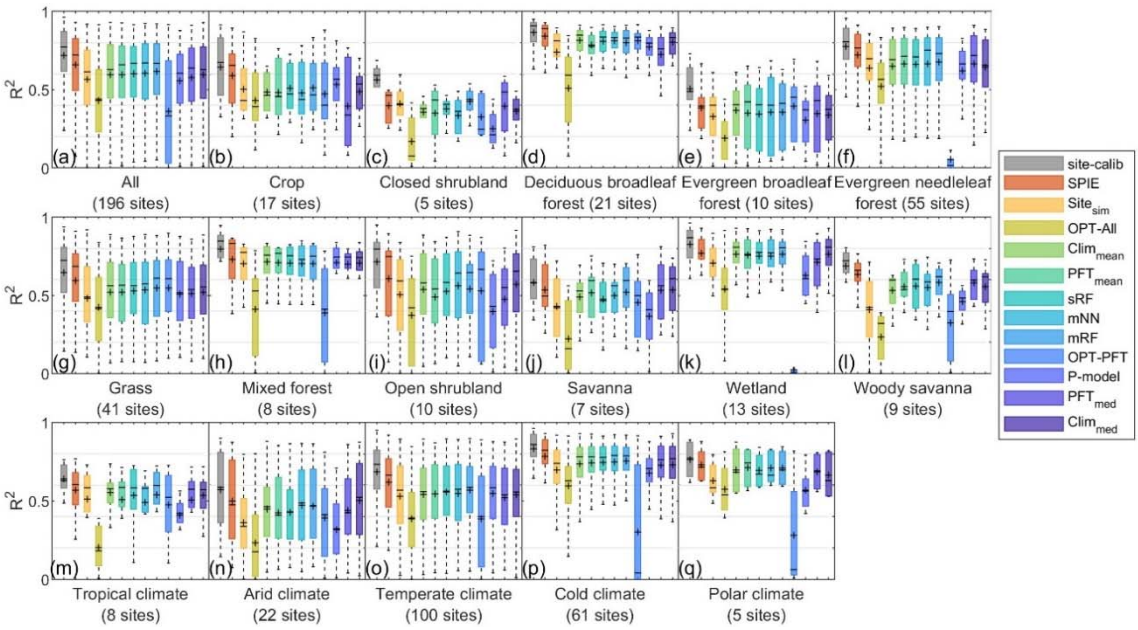

Figure S4. Site-level daily R^2 comparison across all sites (a), per PFT (b-l) and per Clim (m-q). The mean and median per type are represented by the black cross and line, respectively

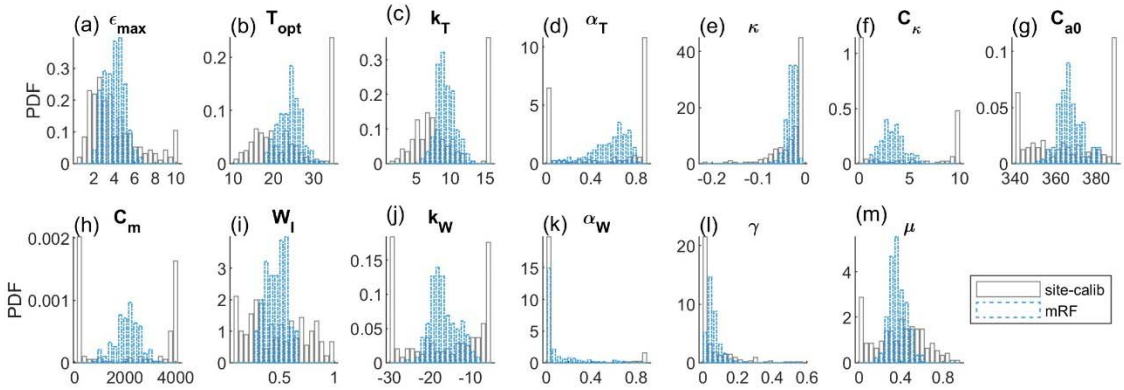

Figure S5. The probability distribution function (PDF) of the predicted parameters by mRF (Upscal) and the calibrated parameters (Calib)

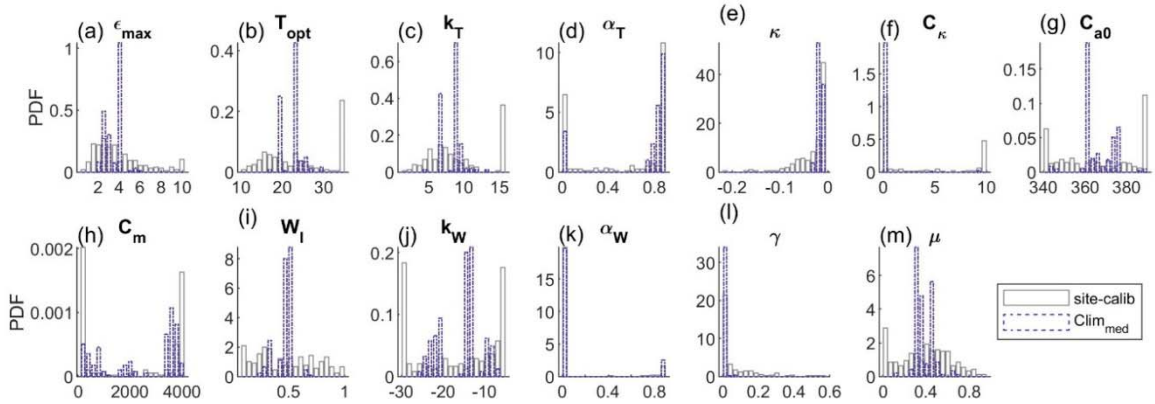

Figure S6. The probability distribution function (PDF) of the predicted parameters by $Clim_{med}$ and the calibrated parameters

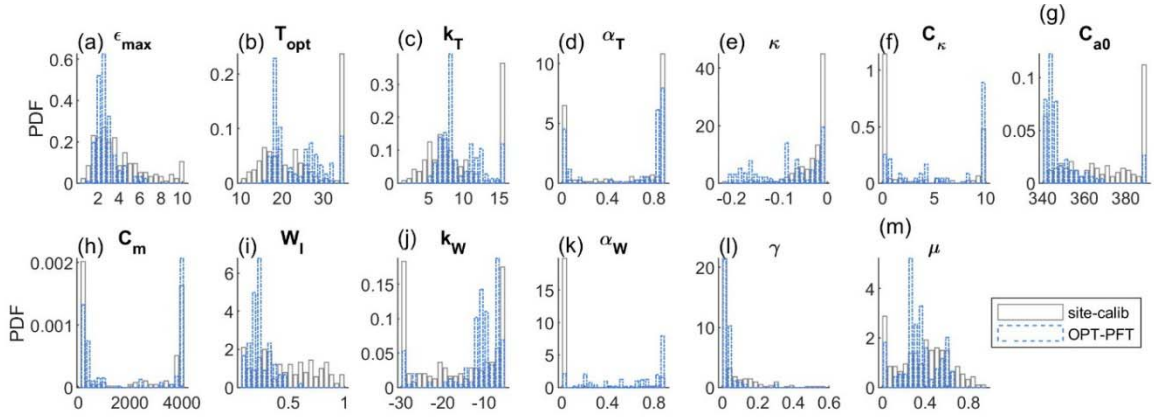

Figure S7. The probability distribution function (PDF) of the predicted parameters by OPT-PFT and the calibrated parameters

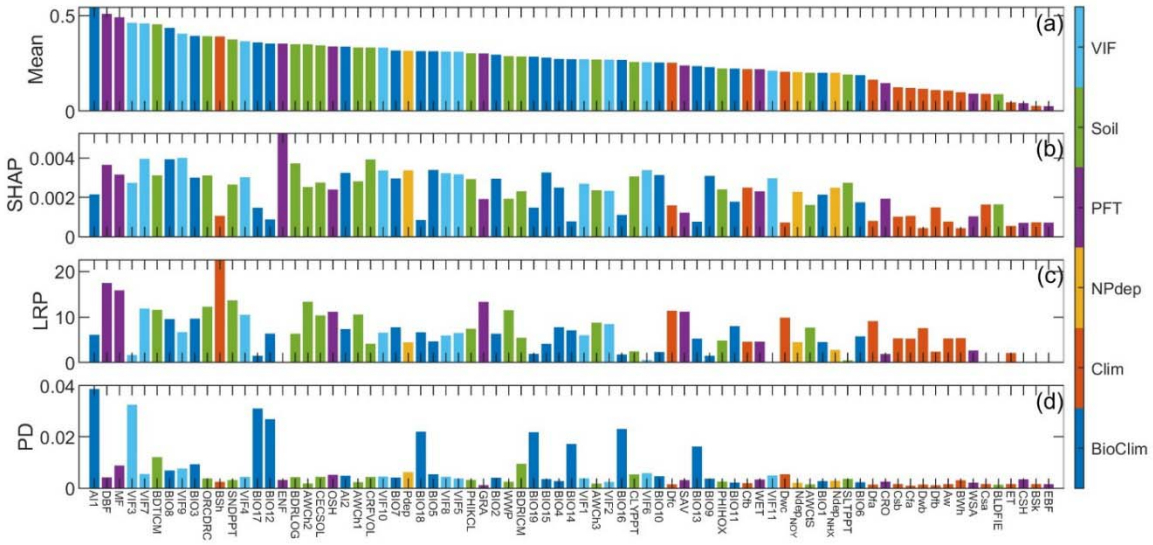

Figure S8. The input features for predicting LUE model parameters sorted according to the average normalized SHAP, LRP and PD values (a). The absolute SHAP, LRP and PD of each feature are shown in b-d in the same order.

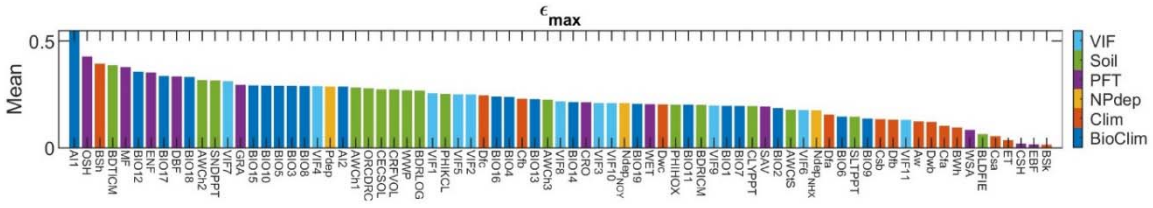

Figure S9. The features sorted by the average normalized SHAP, LRP and PD for ε_{max}

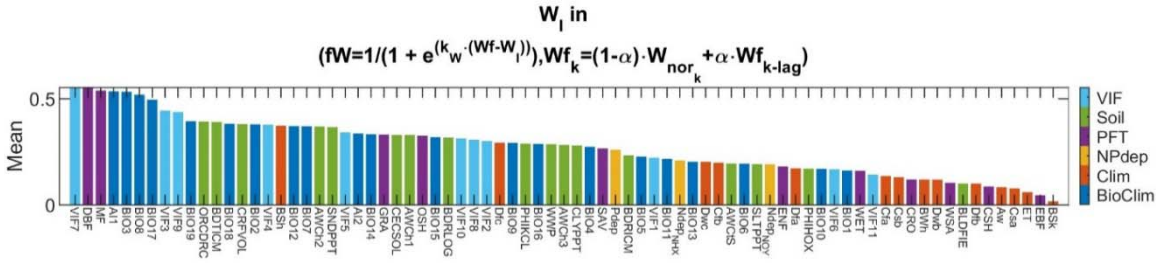

Figure S10. The features sorted by the average normalized SHAP, LRP and PD for W_I

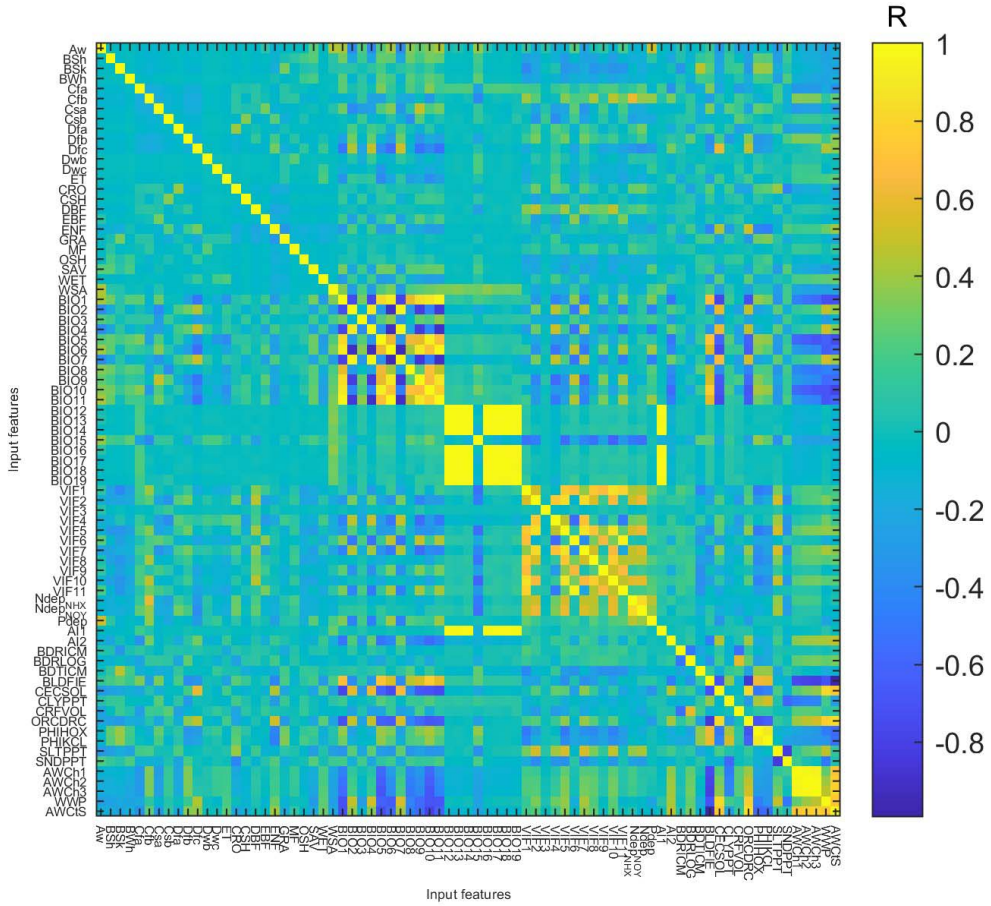

Figure S11. Correlation coefficient (R) matrix between input features.

Table S1. Eddy covariance flux site list used in this study. The latitude (Lat), longitude (Lon) and plant functional types (PFT) are collected from FLUXNET website. The data length differs across site and is determined by the years between 'data start' and 'data end'. The climate type is extracted from the Koeppen-Geiger climate classification map (at 5 arc min; Rubel et al., 2017). The elevation is collected from the site ancillary information, papers and satellite images (see the footnote below the table). The site group refers to the group number of each site used to validate the training result.

SiteID	Lat	Lon	Data start (year)	Data end (year)	PFT	Climate type	Elevation (m)	Site group	Reference
AR-SLu	-33.5	-66.5	2010	2011	MF	BSh	506*e	4	(Ulke et al., 2015)
AT-Neu	47.1	11.3	2002	2012	GRA	Dfc	970	10	(Wohlfahrt et al., 2008)
AU-ASM	-22.3	133.3	2010	2014	ENF	BWh	606*b	5	(Cleverly et al., 2013)

AU-Cpr	-34.0	140.6	2010	2014	SAV	BSk	62[*e]	3	(Bloomfield et al., 2018; Meyer et al., 2015)
AU-Cum	-33.6	150.7	2012	2014	EBF	Cfa	20	1	(Renchon et al., 2018)
AU-DaP	-14.1	131.3	2009	2013	GRA	Aw	71[*e]	3	(Hutley et al., 2011)
AU-DaS	-14.2	131.4	2010	2014	SAV	Aw	110	6	(Hutley et al., 2011)
AU-Dry	-15.3	132.4	2008	2014	SAV	Aw	175	5	(Hutley et al., 2011)
AU-Emr	-23.9	148.5	2011	2013	GRA	BSh	170	3	(Schroder, 2014)
AU-Gin	-31.4	115.7	2013	2014	WSA	Csa	51	3	(Beringer et al., 2016)
AU-GWW	-30.2	120.7	2011	2014	SAV	BSh	450	1	(Beringer et al., 2016)
AU-How	-12.5	131.2	2001	2014	WSA	Aw	64	2	(Beringer et al., 2003)
AU-RDF	-14.6	132.5	2011	2013	WSA	Aw	188[*e]	7	(Bristow et al., 2016)
AU-Rig	-36.7	145.6	2011	2014	GRA	Cfa	152	10	(Beringer et al., 2016)
AU-Stp	-17.2	133.4	2008	2014	GRA	BSh	250[*b]	1	(Hutley et al., 2011)
AU-TTE	-22.3	133.6	2012	2014	OSH	BWh	553	3	(Cleverly et al., 2016)
AU-Tum	-35.7	148.2	2001	2014	EBF	Cfb	1200	8	(Leuning et al., 2005)
AU-Wom	-37.4	144.1	2010	2014	EBF	Cfb	705	6	(Griebel et al., 2016)
AU-Ync	-35.0	146.3	2012	2014	GRA	BSk	126[*e]	6	(Yee et al., 2015)
BE-Bra	51.3	4.5	2000	2014	MF	Cfb	16[*a]	7	(Carrara et al., 2004)
BE-Lon	50.6	4.8	2004	2014	CRO	Cfb	167	2	(Aubinet et al., 2009)
BE-Vie	50.3	6.0	2000	2014	MF	Cfb	450[*a]	1	As above
BR-Ban	-9.8	-50.2	2003	2006	EBF	Aw	120	6	(Da Rocha et al., 2009)
BR-Sp1	-21.6	-47.7	2001	2002	WSA	Aw	690	9	As above
BW-Ma1	-19.9	23.6	2000	2001	WSA	BSh	950	4	(Veenendaal et al., 2004)

CA-Ca1	49.9	-125.3	2000	2005	ENF	Cfb	300	7	(Humphreys et al., 2006)
CA-Ca2	49.9	-125.3	2000	2005	ENF	Csb	300	7	As above
CA-Ca3	49.5	-124.9	2001	2005	ENF	Csb	300	7	As above
CA-Gro	48.2	-82.2	2003	2014	MF	Dfb	340	9	(Pejam et al., 2006)
CA-Let	49.7	-112.9	2000	2005	GRA	BSk	960	7	(Flanagan et al., 2002)
CA-Mer	45.4	-75.5	2000	2005	WET	Dfb	70	1	(Lafleur et al., 2003)
CA-NS2	55.9	-98.5	2002	2005	ENF	Dfc	260	6	(Beringer et al., 2011)
CA-NS3	55.9	-98.4	2001	2005	ENF	Dfc	260	10	As above
CA-NS4	55.9	-98.4	2002	2005	ENF	Dfc	260	6	As above
CA-NS5	55.9	-98.5	2002	2005	ENF	Dfc	260	2	As above
CA-NS6	55.9	-99.0	2001	2005	OSH	Dfc	244	2	As above
CA-NS7	56.6	-100.0	2002	2005	OSH	Dfc	297	5	As above
CA-Oas	53.6	-106.2	2000	2010	DBF	Dfc	530	6	(Black et al., 1996)
CA-Obs	54.0	-105.1	2000	2010	ENF	Dfc	628.94	7	(Jarvis et al., 1997)
CA-Ojp	53.9	-104.7	2000	2005	ENF	Dfb	579	1	(Baldocchi et al., 1997)
CA-Qcu	49.3	-74.0	2001	2006	ENF	Dfb	392.3	4	(Giasson et al., 2006)
CA-Qfo	49.7	-74.3	2004	2010	ENF	Dfc	382	7	(Bergeron et al., 2007)
CA-SF1	54.5	-105.8	2003	2006	ENF	Dfc	536	10	(Mkhabela et al., 2009)
CA-SF2	54.3	-105.9	2001	2005	ENF	Dfc	520	6	As above
CA-SF3	54.1	-106.0	2001	2005	OSH	Dfc	540	5	As above
CA-SJ1	53.9	-104.7	2001	2005	ENF	Dfb	580	8	(Howard et al., 2004)
CA-SJ2	53.9	-104.7	2003	2005	ENF	Dfc	580	1	(Coursolle et al., 2012)
CA-TP1	42.7	-80.6	2008	2014	ENF	Dfb	265	4	(Peichl & Arain, 2007)
CA-TP3	42.7	-80.4	2008	2014	ENF	Dfb	184	2	As above

CA-TP4	42.7	-80.4	2008	2014	ENF	Dfb	184	8	(Arain & Restrepo-Coupe, 2005)
CA-TPD	42.6	-80.6	2012	2014	DBF	Dfb	260	1	As above
CA-WP1	55.0	-112.5	2003	2005	WET	Dfc	540	4	(Syed et al., 2006)
CH-Cha	47.2	8.4	2005	2014	GRA	Cfb	393	5	(Lutz Merbold et al., 2014)
CH-Dav	46.8	9.9	2000	2014	ENF	ET	1639	9	(Wolf et al., 2013; Zielis et al., 2014)
CH-Fru	47.1	8.5	2005	2014	GRA	Cfb	982	3	(Imer et al., 2013)
CH-Oe1	47.3	7.7	2002	2008	GRA	Cfb	450	3	(Ammann et al., 2009)
CN-Cha	42.4	128.1	2003	2005	MF	Dwb	738	1	(Zhang et al., 2006)
CN-Cng	44.6	123.5	2007	2010	GRA	BSk	171[*d]	10	(Pastorello et al., 2020)
CN-Dan	30.5	91.1	2004	2005	GRA	Dwc	4286	8	(Shi et al., 2006)
CN-Du2	42.1	116.3	2006	2008	GRA	Dwb	1350[*b]	5	(Chen et al., 2009)
CN-Ha2	37.6	101.3	2003	2005	WET	Dwc	3357	2	(Pastorello et al., 2020)
CN-Xfs	44.1	116.3	2004	2006	GRA	BSk	1250	4	(Chen et al., 2009)
CZ-BK1	49.5	18.5	2004	2014	ENF	Dfb	908[*a]	8	(Krupková et al., 2017)
CZ-BK2	49.5	18.5	2009	2012	GRA	Dfb	855	7	(Acosta et al., 2013)
CZ-wet	49.0	14.8	2007	2014	WET	Cfb	426	3	(Dušek et al., 2012)
DE-Geb	51.1	10.9	2001	2014	CRO	Cfb	161.5	7	(Anthoni et al., 2004b)
DE-Gri	51.0	13.5	2004	2014	GRA	Cfb	385	4	(Prescher et al., 2010)
DE-Hai	51.1	10.5	2000	2009	DBF	Cfb	430[*a]	9	(Knohl et al., 2003)
DE-Har	47.9	7.6	2005	2006	ENF	Cfb	201	1	(Pastorello et al., 2020)

DE-Kli	50.9	13.5	2004	2014	CRO	Cfb	478	8	(Prescher et al., 2010)
DE-Lnf	51.3	10.4	2002	2012	DBF	Cfb	451	9	(Anthoni et al., 2004a)
DE-Meh	51.3	10.7	2003	2006	MF	Cfb	293[*a]	7	(DON et al., 2009)
DE-Obe	50.8	13.7	2008	2014	ENF	Cfb	734	4	(Pastorello et al., 2020)
DE-SfN	47.8	11.3	2013	2014	WET	Cfb	590	2	(Hommeltenberg et al., 2014)
DE-Tha	51.0	13.6	2000	2014	ENF	Cfb	380[*a]	3	(Bernhofer et al., 2003)
DE-Wet	50.5	11.5	2002	2006	ENF	Cfb	785[*a]	8	(Rebmann et al., 2010)
DK-Ris	55.5	12.1	2004	2005	CRO	Cfb	10	10	(Pastorello et al., 2020)
DK-Sor	55.5	11.6	2000	2014	DBF	Cfb	40[*a]	10	(Pilegaard & Ibrom, 2020)
ES-Amo	36.8	-2.3	2000	2014	OSH	BSh	58	3	(López-Ballesteros et al., 2017)
ES-ES1	39.4	-0.3	2007	2012	ENF	Csa	5[*a]	3	(Sanz M J, 2004)
ES-ES2	39.3	-0.3	2000	2006	CRO	Csa	10	9	As above
ES-LgS	37.1	-3.0	2004	2006	OSH	Csb	2267	9	(Reverter et al., 2010)
ES-LJu	36.9	-2.8	2005	2011	OSH	Csa	1600	6	(Serrano-Ortiz et al., 2009)
ES-LMa	39.9	-5.8	2004	2006	SAV	Csa	258[*a]	5	(Perez-Priego et al., 2017)
ES-VDA	42.2	1.5	2007	2009	GRA	Cfb	1765[*a]	2	(Pastorello et al., 2020)
FI-Hyy	61.9	24.3	2004	2006	ENF	Dfc	181[*a]	8	(Suni et al., 2003)
FI-Kaa	69.1	27.3	2000	2014	WET	Dfc	155	2	(MIKA AURELA et al., 2007)
FI-Let	60.6	24.0	2000	2006	ENF	Dfb	111	5	(Koskinen et al., 2014)
FI-Lom	68.0	24.2	2009	2012	WET	Dfc	269[*a]	2	(M. Aurela et al., 2015)

FI-Sod	67.4	26.6	2007	2009	ENF	Dfc	180[*a]	1	(Thum et al., 2007)
FR-Fon	48.5	2.8	2008	2014	DBF	Cfb	92[*a]	8	(Michelot et al., 2011)
FR-Gri	48.8	2.0	2005	2013	CRO	Cfb	125	6	(Loubet et al., 2011)
FR-Hes	48.7	7.1	2004	2014	DBF	Cfb	300[*a]	2	(Granier et al., 2000)
FR-LBr	44.7	-0.8	2000	2006	ENF	Cfb	61[*a]	1	(Berbigier et al., 2001)
FR-Lq1	45.6	2.7	2000	2008	GRA	Cfb	1040	9	(Pastorello et al., 2020)
FR-Lq2	45.6	2.7	2004	2006	GRA	Cfb	1040	1	(Pastorello et al., 2020)
FR-Pue	43.7	3.6	2004	2006	EBF	Csa	270[*a]	5	(Rambal et al., 2004)
GL-ZaH	74.5	-20.6	2000	2014	GRA	ET	48	4	(Lund et al., 2012)
HU-Bug	46.7	19.6	2002	2006	GRA	Cfb	111[*a]	7	(Pastorello et al., 2020)
IL-Yat	31.3	35.1	2001	2006	ENF	Csa	650	7	(Tatarinov et al., 2016)
IT-Amp	41.9	13.6	2002	2006	GRA	Cfb	884[*a]	6	(Papale et al., 2015)
IT-BCi	40.5	15.0	2004	2012	CRO	Csa	20	7	(Vitale et al., 2016)
IT-CA1	42.4	12.0	2011	2014	DBF	Csa	200	4	(Sabbatini et al., 2016)
IT-CA2	42.4	12.0	2011	2014	CRO	Csa	200	5	(Sabbatini et al., 2016)
IT-CA3	42.4	12.0	2011	2014	DBF	Csa	197	5	(Sabbatini et al., 2016)
IT-Col	41.9	13.6	2004	2014	DBF	Cfb	1560[*a]	4	(VALENTINI et al., 1996)
IT-Cpz	41.7	12.4	2000	2008	EBF	Csa	68	8	(Tirone et al., 2003)
IT-Isp	45.8	8.6	2013	2014	DBF	Cfa	210	9	(Ferréa et al., 2012)
IT-Lav	46.0	11.3	2004	2014	ENF	Cfb	1353	2	(B. Marcolla et al., 2003)
IT-Lec	43.3	11.3	2005	2006	EBF	Csa	314	8	(Pastorello et al., 2020)

IT-MBo	46.0	11.1	2003	2013	GRA	Dfb	1550[*a]	5	(Barbara Marcolla et al., 2005)
IT-Noe	40.6	8.2	2004	2014	CSH	Csa	25	10	(Papale et al., 2015)
IT-Non	44.7	11.1	2001	2006	MF	Cfa	25[*c]	1	(Nardino, 2002)
IT-PT1	45.2	9.1	2002	2004	DBF	Cfa	60	8	(Migliavacca et al., 2009)
IT-Ren	46.6	11.4	2002	2013	ENF	Dfc	1730[*a]	10	(Barbara Marcolla et al., 2005)
IT-Ro1	42.4	11.9	2000	2008	DBF	Csa	235	9	(Rey et al., 2002)
IT-Ro2	42.4	11.9	2002	2012	DBF	Csa	224[*a]	4	(TEDESCHI et al., 2006)
IT-SR2	43.7	10.3	2013	2014	ENF	Csa	4	10	(Pastorello et al., 2020)
IT-SRo	43.7	10.3	2000	2012	ENF	Csa	4[*a]	7	(Chiesi et al., 2005)
IT-Tor	45.8	7.6	2008	2012	GRA	ET	2160	10	(Galvagno et al., 2013)
NL-Ca1	52.0	4.9	2003	2006	GRA	Cfb	0.7	3	(Jacobs et al., 2007)
NL-Loo	52.2	5.7	2000	2014	ENF	Cfb	25[*a]	9	(Dolman et al., 2002)
PT-Cor	39.1	-8.3	2010	2017	EBF	Csa	170[*c]	6	(Pastorello et al., 2020)
PT-Esp	38.6	-8.6	2002	2006	EBF	Csa	95[*a]	9	(Rodrigues et al., 2011)
PT-Mi1	38.5	-8.0	2003	2005	EBF	Csa	264[*a]	10	(Pereira et al., 2007)
PT-Mi2	38.5	-8.0	2004	2006	GRA	Csa	190	8	(Pereira et al., 2007)
RU-Fyo	56.5	32.9	2002	2014	ENF	Dfb	265[*a]	9	(Kurbatova et al., 2008)
RU-Ha1	54.7	90.0	2002	2004	GRA	Dfb	446	4	(Belelli Marchesini et al., 2007)
RU-Zot	60.8	89.4	2002	2004	ENF	Dfc	90	10	(Arneth et al., 2002)
SD-Dem	13.3	30.5	2007	2009	SAV	BWh	500	2	(Ardö et al., 2008)

SE-Deg	64.2	19.6	2001	2005	WET	Dfc	270	6	(Sagerfors et al., 2008)
SE-Fla	64.1	19.5	2000	2002	ENF	Dfc	226[*c]	3	(Valentini et al., 2000)
US-AR1	36.4	-99.4	2009	2012	GRA	Cfa	611	6	(Billesbach D, 2016)
US-AR2	36.6	-99.6	2009	2012	GRA	Cfa	646	10	(Billesbach D, 2016)
US-ARb	35.6	-98.0	2003	2012	GRA	Cfa	424	8	(Pastorello et al., 2020)
US-ARc	35.6	-98.0	2005	2006	GRA	Cfa	424	5	(Pastorello et al., 2020)
US-ARM	36.6	-97.5	2005	2006	CRO	Cfa	314	2	(Pastorello et al., 2020)
US-Atq	70.5	-157.4	2003	2008	WET	ET	15	10	(Pastorello et al., 2020)
US-Aud	31.6	-110.5	2002	2006	GRA	BSk	1469	9	(Pastorello et al., 2020)
US-Bar	44.1	-71.3	2004	2005	DBF	Dfb	272	8	(Ouimette et al., 2018)
US-Bkg	44.4	-96.8	2004	2006	GRA	Dfa	510	4	(Gilmanov et al., 2005)
US-Blo	38.9	-120.6	2000	2007	ENF	Csb	1315	1	(Goldstein et al., 2000)
US-Bo1	40.0	-88.3	2000	2007	CRO	Cfa	219	2	(Pastorello et al., 2020)
US-Bo2	40.0	-88.3	2004	2006	CRO	Cfa	219	9	(Pastorello et al., 2020)
US-Cop	38.1	-109.4	2011	2013	GRA	BSk	1520	1	(D., 2016)
US-CRT	41.6	-83.4	2001	2007	CRO	Dfa	180	8	(Pastorello et al., 2020)
US-Dk1	36.0	-79.1	2001	2005	GRA	Cfa	168	7	(Pastorello et al., 2020)
US-Dk3	36.0	-79.1	2001	2005	ENF	Cfa	163	4	(Pastorello et al., 2020)

US-Fmf	35.1	-111.7	2000	2006	ENF	Csb	2160	5	(Pastorello et al., 2020)
US-FPe	48.3	-105.1	2004	2006	GRA	BSk	634	3	(Pastorello et al., 2020)
US-FR2	30.0	-98.0	2005	2006	WSA	Cfa	271.9	5	(Heinsch et al., 2004)
US-Goo	34.3	-89.9	2002	2006	GRA	Cfa	87	10	(T., 2016)
US-Ha1	42.5	-72.2	2000	2012	DBF	Dfb	340	2	(Urbanski et al., 2007)
US-Ho1	45.2	-68.7	2000	2004	ENF	Dfb	60	10	(Hollinger et al., 1999)
US-IB1	41.9	-88.2	2005	2007	CRO	Dfa	226.5	3	(Pastorello et al., 2020)
US-IB2	41.8	-88.2	2004	2011	GRA	Dfa	226.5	5	(Pastorello et al., 2020)
US-Ivo	68.5	-155.8	2004	2007	WET	ET	568	1	(Epstein et al., 2004)
US-KS2	28.6	-80.7	2003	2006	CSH	Cfa	3	6	(Powell et al., 2006)
US-Los	46.1	-90.0	2000	2014	WET	Dfb	480	4	(Sulman et al., 2009)
US-Me2	44.5	-121.6	2000	2014	ENF	Csb	1253	2	(Kwon et al., 2018; Thomas et al., 2009)
US-Me3	44.3	-121.6	2004	2006	ENF	Csb	1005	6	(Vickers et al., 2012)
US-Me5	44.4	-121.6	2002	2014	ENF	Csb	1188	4	(Law et al., 2001; Williams et al., 2001)
US-Me6	44.3	-121.6	2004	2009	ENF	Csb	998	7	(Ruehr et al., 2014)
US-MMS	39.3	-86.4	2000	2002	DBF	Cfa	275	7	(Roman et al., 2015)
US-MOz	38.7	-92.2	2010	2014	DBF	Cfa	219.4	3	(Gu et al., 2016)
US-Myb	38.1	-121.8	2011	2014	WET	Csa	-1	2	(Pastorello et al., 2020)
US-NC1	35.8	-76.7	2005	2006	OSH	Cfa	5	4	(Noormets et al., 2012)

US-NC2	35.8	-76.7	2005	2006	ENF	Cfa	5	2	(Pastorello et al., 2020)
US-Ne1	41.2	-96.5	2000	2014	CRO	Dfa	361	7	(Pastorello et al., 2020)
US-Ne2	41.2	-96.5	2001	2013	CRO	Dfa	362	8	(Pastorello et al., 2020)
US-Ne3	41.2	-96.4	2001	2013	CRO	Dfa	363	6	(Pastorello et al., 2020)
US-NR1	40.0	-105.6	2001	2013	ENF	Dfc	3050	9	(Monson et al., 2002)
US-Oho	41.6	-83.8	2004	2013	DBF	Dfa	230	4	(DeForest et al., 2006)
US-Prr	65.1	-147.5	2011	2014	ENF	Dfc	210	3	(Ikawa et al., 2015; Nakai et al., 2013)
US-SO2	33.4	-116.6	2004	2006	CSH	Csb	1394	3	(Lipson et al., 2005)
US-SO3	33.4	-116.6	2001	2006	CSH	Csb	1429	5	(Lipson et al., 2005)
US-SO4	33.4	-116.6	2004	2006	CSH	Csb	1429	5	(Lipson et al., 2005)
US-SP2	29.8	-82.2	2000	2004	ENF	Cfa	50	9	(Clark et al., 1999)
US-SP3	29.8	-82.2	2000	2004	ENF	Cfa	50	6	(Clark et al., 1999)
US-SRC	31.9	-110.8	2008	2014	OSH	BSh	991	6	(Pastorello et al., 2020)
US-SRG	31.8	-110.8	2008	2014	GRA	Csa	1291	2	(Scott et al., 2015)
US-SRM	31.8	-110.9	2004	2014	WSA	BSk	1120	5	(Scott et al., 2009)
US-Syv	46.2	-89.4	2001	2014	MF	Dfb	540	6	(Desai et al., 2005)
US-Ton	38.4	-121.0	2001	2014	WSA	Csa	177	8	(Ma et al., 2016)
US-Twt	38.1	-121.7	2009	2014	CRO	Csa	-7	5	(Pastorello et al., 2020)
US-UMB	45.6	-84.7	2000	2014	DBF	Dfb	234	10	(Gough et al., 2008)
US-Var	38.4	-121.0	2000	2014	GRA	Csa	129	9	(Ma et al., 2011)

US-WCr	45.8	-90.1	2000	2014	DBF	Dfb	520	4	(Cook et al., 2004)
US-Whs	31.7	-110.1	2011	2013	OSH	BSk	1370	10	(Pastorello et al., 2020)
US-Wi4	46.7	-91.2	2007	2014	ENF	Dfb	352	7	(Noormets et al., 2007)
US-Wi9	46.6	-91.1	2002	2005	ENF	Dfb	350	1	(Noormets et al., 2007)
US-Wkg	31.7	-109.9	2004	2005	GRA	BSk	1531	8	(Scott, 2010)
US-WPT	41.5	-83.0	2004	2014	WET	Cfa	175	3	(Pastorello et al., 2020)
US-Wrc	45.8	-122.0	2000	2006	ENF	Csb	371	1	(Wharton et al., 2012)
ZA-Kru	-25.0	31.5	2000	2012	SAV	BSh	359	3	(Archibald et al., 2009)
ZM-Mon	-15.4	23.3	2007	2009	WSA	Aw	1053	9	(L. Merbold et al., 2009)

Note.

[*a]: collected from (Flechard et al., 2020).

[*b]: collected from (Hao et al., 2019).

[*c]: collected from (B. Tang et al., 2018).

[*d]: collected from (X. Tang et al., 2020).

[*e]: extracted from google earth.

Other elevation data were collected from https://fluxnet.org/, http://www.europe-fluxdata.eu/, http://www.ozflux.org.au/, https://ameriflux.lbl.gov/, http://www.asiaflux.net/, http://www.chinaflux.org/, and ancillary information of LaThuile dataset (https://fluxnet.org/data/la-thuile-dataset/).

131 **Table S2.** List of the forcing variables for the LUE model. The variables in bold are used to
132 calibrate the model parameters.

Abbreviation	Definition	Unit	Equation or source	Reference
LE	Latent heat flux, 'LE_F_MDS' in FLUXNET2015 dataset or 'LE_f' in LaThuile dataset	$MJ·m^{-2}·d^{-1}$	EC observations	See Table S1
NEE	Net ecosystem exchange, 'NEE_VUT_REF' or 'NEE_f'	$gC·m^{-2}·d^{-1}$	EC observations	
Precip	Precipitation, 'P_F' or 'precip'	mm	EC observations	

QA	Quality flag of the variable from EC measurement, e.g., 'SW_IN_F_QC' is the QA of global radiation in FLUXNET2015 dataset, and 'Rg_fqcOK' is QA of that in LaThuile dataset.	Unitless (0-1)	FLUXNET dataset	(Pastorello et al., 2020)
QC	Quality flags for all the reflectance of MCD43A4 product	Unitless	MCD43A2 quality assessment product	(Schaaf & Wang, 2015)
R_g[a]	Global radiation, 'SW_IN_F' or 'Rg_f'	MJ·m^{-2}·d^{-1}	EC observations	
R_p[a]	Potential radiation, 'SW_IN_POT' or 'Rg_pot'	MJ·m^{-2}·d^{-1}	EC observations	See Table S1
R_n[a]	Net radiation, 'NETRAD' or 'Rn_f'	MJ·m^{-2}·d^{-1}	EC observations	
r_{red}	Reflectance at red band	Unitless (0-1)	MCD43A4 version 6 Nadir BRDF-Adjusted Reflectance product	(Schaaf & Wang, 2015)
r_{nir}	Reflectance at near-infrared band	Unitless (0-1)	As above	
T[a]	Air temperature, 'TA_F' or 'Tair_f'	°C	EC observations	See Table S1
VPD[a]	Vapor pressure deficit, 'VPD_F' or 'VPD_f'	kPa	EC observations	See Table S1
CI	Cloudiness index	Unitless (0-1)	$1-R_g/R_p$	(Fu & Rich, 1999; Turner et al., 2006)
CO_2	Atmospheric CO_2 concentration	ppm	Observations by NOAA/ESRL. The global annual mean atmospheric CO_2 concentration was converted to daily time steps using a linear interpolation function	www.esrl.noaa.gov/gmd/ccgg/trends/
ET_{obs}[d]	Evapotranspiration	mm	converted from LE using a latent heat of vaporization changing with T	(Henderson - Sellers, 1984)
PET	Potential ET	mm	Estimated using Rn and T	(Priestley & Taylor, 1972)

GPP_{obs}[d]	Gross primary productivity, 'GPP_NT_VUT_REF' or 'GPP_f'	$gC·m^{-2}·d^{-1}$	Estimated from NEE using the night-time partitioning method	(Reichstein et al., 2005)
NDVI[c]	MODIS-based Normalized differential vegetation index	Unitless (-1-1)	$\frac{r_{nir}-r_{red}}{r_{nir}+r_{red}}$	(Rouse et al., 1974)
PAR	Photosynthetically active radiation	$MJ·m^{-2}·d^{-1}$	$R_g \times 0.45$	(Running & Zhao, 2015; Weiss & Norman, 1985)
WAI	Water availability index	mm	Estimated using Precip and PET, with two site-level calibrated parameters	See the algorithm of WAI in (Boese et al., 2019; Tramontana et al., 2016) and detailed calibration process in section S1 in (Bao et al., 2022)
W	Soil water supply	Unitless (0-1)	$W = \min(1, WAI/AWC)$	(Bao et al., 2022)
σ_{LE}	Random uncertainty of ET, 'LE_RANDUNC' or 'LE_fsd_UncNew_fullDay_m1'	$MJ·m^{-2}·d^{-1}$	Standard deviation of LE	(Pastorello et al., 2020)
σ_{NEE}	Random uncertainty of GPP, 'NEE_VUT_REF_RANDUNC' or 'NEE_fsd_UncNew_fullDay_m1'	$gC·m^{-2}·d^{-1}$	Standard deviation of NEE	
FAPAR[b]	Fraction of absorbed PAR	Unitless (0-1)	$\begin{cases} = NDVI\ (NDVI>0) \\ = 0\ (NDVI\leq 0) \end{cases}$	(Myneni et al., 1997)

Note. All the above variables are at the daily scale;

[a]The gaps in the R_g, R_p, R_n, T, and VPD were filled using machine-learning-based downscaling (Besnard et al., 2019) of gridded product from CRUNCEP (Viovy, 2018);

[b]The linear relationship between FAPAR and NDVI was assumed according to (Myneni et al., 1997).

[c]The gaps in NDVI was filled using FluxnetEO dataset (Walther et al., 2022). The time-series NDVI were filtered by Savitzky-Golay filter (window size was eleven and polynomial order was three) (Savitzky & Golay, 1964).

[d]Since GPP_{obs} is estimated from NEE and ET_{obs} is estimated from LE, the QA of GPPobs and ETobs are represented by QA of NEE ('NEE_VUT_REF_QC' or 'NEE_fsd_UncNew_fullDay_m1') and LE ('LE_F_MDS_QC' or 'LE_fsd_UncNew_fullDay_m1'), respectively.

133 **Table S3.** Eddy covariance flux site list used in this study. The latitude (Lat), longitude (Lon)
134 and plant functional types (PFT) are collected from FLUXNET website. The data length differs

across site and is determined by the years between 'data start' and 'data end'. The climate type is extracted from the Koeppen-Geiger climate classification map (at 5 arc min; Rubel et al., 2017). The elevation is collected from the site ancillary information, papers and satellite images (see the footnote below the table). The site group refers to the group number of each site used to validate the training result.

Class name	Short names	Definitions	References
PFT	PFT	Plant functional types	See Table S1, eleven types in total
Clim	Clim	Koeppen-Geiger climate classification types	See Table S1, five main climate types and fourteen specific classification types in total
BioClim	BIO1	Annual Mean Temperature	Calculated based on the ANUCLIM algorithm (Xu & Hutchinson, 2011) using CRUNCEP dataset (Viovy, 2018) from 1986-2015.
	BIO2	Mean Diurnal Range (Mean of monthly maximum temperature minus minimum temperature)	
	BIO3	Isothermality (BIO2 divided by BIO7 and 100)	
	BIO4	Temperature Seasonality (standard deviation of temperature multiply with 100)	
	BIO5	Max Temperature of Warmest Month	
	BIO6	Min Temperature of Coldest Month	
	BIO7	Temperature Annual Range (BIO5 minus BIO6)	
	BIO8	Mean Temperature of Wettest Quarter	
	BIO9	Mean Temperature of Driest Quarter	
	BIO10	Mean Temperature of Warmest Quarter	
	BIO11	Mean Temperature of Coldest Quarter	
	BIO12	Annual Precipitation	
	BIO13	Precipitation of Wettest Month	
	BIO14	Precipitation of Driest Month	
	BIO15	Precipitation Seasonality (Coefficient of Variation)	
	BIO16	Precipitation of Wettest Quarter	
	BIO17	Precipitation of Driest Quarter	
	BIO18	Precipitation of Warmest Quarter	
	BIO19	Precipitation of Coldest Quarter	
	AI1	Mean annual aridity index (ratio between mean annual precipitation and potential evapotranspiration)	Calculated using the CRUNCEP dataset from 1986-2015
	AI2	Seasonality of aridity index (standard deviation of mean monthly aridity index)	

VIF	VIF1	Annual mean EVI (enhanced vegetation index)	Calculated based on the bioclimatic variables (BIO1-BIO11) algorithm using the gap-filled Landsat-based EVI (Walther et al., 2022) from 1986-2015
	VIF2	Mean monthly EVI range	
	VIF3	Mean EVI variability (VIF2 divided by VIF7)	
	VIF4	EVI seasonality (standard deviation of EVI)	
	VIF5	Max EVI of Warmest Month	
	VIF6	Min EVI of Coldest Month	
	VIF7	Annual EVI Range (BIO5 minus BIO6)	
	VIF8	Mean EVI of Wettest Quarter	
	VIF9	Mean EVI of Driest Quarter	
	VIF10	Mean EVI of Warmest Quarter	
	VIF11	Mean EVI of Coldest Quarter	
NPdep	$Ndep_{NHX}$	Average atmospheric nitrogen deposition (NH_3 and NH_4)	Extracted from the product of the atmospheric chemistry transport model TM3 (Wang et al., 2017)
	$Ndep_{NOY}$	Average atmospheric nitrogen deposition (NO and NO_2)	
	Pdep	Average atmospheric phosphorus deposition	
Soil	BDRICM	Depth to bedrock (R horizon) up to 200 cm	Extracted from the Soil Grids product (Poggio et al., 2021)
	BDRLOG	Probability of occurrence (0-100%) of R horizon	
	BDTICM	Absolute depth to bedrock (in cm)	
	BLDFIE	Bulk density (fine earth) in kg/m3 at depth 0.00 m	
	CECSOL	Cation exchange capacity of soil in cmol/kg at depth 0.00 m	
	CLYPPT	Clay content (0-2 micro meter) mass fraction in % at depth 0.00 m	
	CRFVOL	Coarse fragments volumetric in % at depth 0.00 m	
	ORCDRC	Soil organic carbon content (fine earth fraction) in g/kg at depth 0.00 m	
	PHIHOX	Soil pH*10 in H2O at depth 0.00 m	
	PHIKCL	Soil PH*10 in KCl at depth 0.00 m	
	SLTPPT	Silt content (2-50 micro meter) mass fraction in % at depth 0.00 m	
	SNDPPT	Sand content (50-2000 micro meter) mass fraction in % at depth 0.00 m	
	AWCh1	Derived available soil water capacity (volumetric fraction) with FC = pF 2.0 for	

	depth 0 cm
AWCh2	Derived available soil water capacity (volumetric fraction) with FC = pF 2.3 for depth 0 cm
AWCh3	Derived available soil water capacity (volumetric fraction) with FC = pF 2.5 for depth 0 cm
WWP	Derived available soil water capacity (volumetric fraction) until wilting point for depth 0 cm
AWCtS	Saturated water content (volumetric fraction) teta-S for depth 0 cm

140